# Supporting Information

## Open the Sodalite Cages of X Zeolite for Boosting Toluene Side-Chain Alkylation Performance

Zhe Hong [a, *], Lei Li [a], Lei Miao [b], Guoqing Zhao [c], Zhirong Zhu [b, *]

[a] *College of Biological, Chemical Sciences and Engineering, Jiaxing University, Jiaxing, Zhejiang, 314001, China;*

[b] *School of Chemical Science and Engineering, Tongji University, Shanghai 200092, China;*

[c] *College of Chemical and Material, Fudan University, Shanghai 200433, China;*

*Corresponding author

E-mail address: 1961268317@qq.com; zhuzhirong@tongji.edu.cn

# Table of Contents



**List of Tables, Scheme and Figures**

corresponding to supercages.

Figure S5. The IR spectra of dehydrated (a) X-FT-30 and (b) X-FT-60 samples.

Figure S6. (a) CI values and (b) *n*-hexane cracking rates on X-P and derivatives $NH_4F$ treated for 15, 30, and 60 min.

Figure S7. Conversion of toluene and total selectivity of styrene and ethylbenzene for side-chain alkylation reaction over X-P and X-FT-15 samples. Reaction conditions: 698 K, toluene/methanol ratio = 3.0, WHSV = 2.0 $h^{-1}$.

Figure S8. $CO_2$-TPD profiles of the Cs-X-P, Cs-X-FT-15 and Cs-X-FT-30 catalysts.

Figure S9. Cs $3d_{5/2}$ XPS signals of Cs-X-P, Cs-X-FT-15 and Cs-X-FT-30 catalysts. Each catalyst shows two Cs $3d_{5/2}$ peaks, indicating the existence of two kinds of Cs species: the peak centred at around 722.2 eV was attributed to $Cs^+$, while the other signal ranged from 723.0 to 723.2 eV was assigned to $Cs_2O$ species.

Figure S10. (a) variation of toluene conversion with the flow rate of reactants on Cs-X-FT-15 catalyst (tuning the catalyst mass from 2.5 g to 6.25 g to achieve different reactants flow rates at constant WHSV of 2.0 $h^{-1}$) and (b) variation of toluene reaction rates with the Cs loading on Cs-X-FT-15 catalyst (tuning CsOH concentrations from 0.3M to 0.6 M during Cs ion exchange procedures).

Figure S11. (a) natural log of toluene conversion as a function of the natural log of space time and (b) the dependence of toluene conversion rate on the concentration of styrene products (1.23-5.88 mol%).

**S1. Experimental**

**Samples preparation**

**Fluoride etching.** The commercial NaX zeolite (Nankai University, Si/Al = 1.3) was firstly ion-exchanged with aqueous solution of ammonium chloride three times at 333 K for 4 h, followed by centrifugation, washed with distilled water, and dried overnight at 353 K. Then the resulting $NH_4$-form zeolite was subjected to $NH_4F$ treatment at different temperatures. Typically, it was added to a 0.1 M $NH_4F$ solution (50 mL of solution/10 g of zeolite) and stirred at 200 rpm. This treatment was performed by ultrasonic assisting at 298 K for 15/30/60 min respectively. Subsequently, the solid products were thoroughly washed with distilled water, dried overnight at 353 K and then calcined at 813 K under a dry air flow for 4 h. The resultant zeolite was denoted as X-FT-*n*, where *n* represents the $NH_4F$-treated time with the unit of minute. For comparison, the $NH_4$-X without $NH_4F$-treated was also calcined under the same condition, which denoted as X-P.

The ion-exchange with TMA cations was carried out as follows: 1 g of sample was ion-exchanged at 333 K for 4 h (450 rpm) with a 0.3 M solution of tetramethylammonium chloride (20 mL of solution/1 g of zeolite). Then the resultant sample was filtered and washed with excess pure water and ion exchange process was repeated two times. The final product was thoroughly washed and then dried at 353 K for 6 h. The resultant $TMA^+$-exchanged samples were denoted as *TMA*-X-FT-*n* and *TMA*-X-P.

**Cesium-exchanged zeolite X.** To investigate the catalytic performance of the $NH_4F$-treated X for side-chain alkylation of toluene with methanol, the cesium ion-exchange was carried out as follows: 10 g of sample was ion-exchanged at 333 K for 4 h (450

rpm) with a 0.3 M solution of $CsOH \cdot H_2O$ (50 mL of solution/10 g of zeolite). The resultant sample was filtered and washed thoroughly with excess pure water. The ion-exchange process was repeated three times. The resultant samples was then dried overnight at 353 K and calcined at 813 K under a dry air flow for 4 h. The resultant $Cs^+$-exchanged samples were denoted as Cs-X-FT-*n* and Cs-X-P.

**Characterization**

The X-ray diffraction (XRD) patterns were performed using a Bruker D8 diffractometer with Cu-Kα radiation (λ = 1.5405 Å, 30 kV, 10 mA). The samples were scanned from 2θ of 5-70$^o$ with a step size of 0.02$^o$.

$N_2$ adsorption-desorption isotherms were measured on a Micrometrics ASAP 2020 at 77 K after vacuumizing the sample at 623 K for 4 h. The specific surface area was calculated using the Brunauer-Emmett-Teller (BET) method. Micropore volumes ($V_{micro}$) were determined by *t*-plot method. The total volume was taken from the adsorbed nitrogen volume at $P/P_0 = 0.99$.

Scanning electron microscopy (SEM) images and energy dispersive X-ray spectroscopy (EDS) mapping were taken with a Hitachi S-5500 instrument with an acceleration voltage of 10 kV. Transmission electron microscopy (TEM) images were recorded with Tecnai G2 F20. The samples were dispersed into alcohol before observation.

The elemental compositions of catalysts were measured by inductively coupled plasma optical emission spectroscopy (ICP-AES, OPTIMA-3000).

Infrared (IR) spectrum was recorded on a Thermo Nicolet$^{TM}$ 6700 Fourier-

transform infrared spectroscopy (FT-IR) spectrometer in the region of 400-4000 $cm^{-1}$. The powder of sample was first dehydrated at 673 K for 30 min with a heating ramp of 2 K/min under pure $N_2$ flow (30 ml/min). The FTIR spectrum was collected after the sample cooled down to room temperature. Each spectrum was obtained by averaging 64 scans collected at 1 $cm^{-1}$ resolution. The extinction coefficients used for the quantification of OH groups in supercages (3640 $cm^{-1}$) and sodalite cage (3550 $cm^{-1}$) were $\varepsilon_{3640} = 6.76$ and $\varepsilon_{3550} = 5.39$ cm/μmol.[1] Quantitative IR analysis is based on above extinction coefficients and the Beer-Lambert law.[2]

The thermogravimetric/differential scanning calorimetry (TG/DSC) analysis was carried out in an air atmosphere on the SHIMADZU TGA-50/DSC-60 Plus. The TG curves were collected in the range of 303-1173 K with a heating ramp of 5 K/min, and DSC curves were collected in the range of 303-773 K.

$^{27}Al$ MAS NMR spectroscopy was performed on a Bruker AVANCE III 600 spectrometer at resonance frequencies of 156.4 MHz. The chemical shifts of $^{27}Al$ were referenced to 1 M aqueous $Al(NO_3)_3$. $^{129}Xe$ NMR spectroscopy was performed on a Varian Infinity-Plus 400 spectrometer at resonance frequencies of 110.6 MHz. A gas mixture containing 2% Xe, 2% $N_2$, and 96% He was delivered at the rate of 100 mL/min to the sample in the detection region. The samples were first cooled down to 193 K and then the temperature was elevated to 298 K and kept it for 10 min. All spectra were acquired with 3.0 $\mu s$ $\pi/2$ pulse, 64 scans and a recycle delay of 1 s. The position of gaseous xenon is taken as the reference and fixed at 0 ppm.

X-ray photoelectron spectroscopy (XPS) measurements were performed on

Escalab 250 (Thermo Fisher VG) with a monochromatic X-ray source of Al Kα under ultra-high vacuum ($2.4\times10^{-8}$ Pa). The deconvolution method of XPS spectra was fitted by Gaussian function.

Temperature-programmed desorption (TPD) profiles of $CO_2$ and $NH_3$ were collected on a Micromeritics Autochem2920 instrument in a quartz reactor with a thermal conductivity detector (TCD). 0.1 g of the sample was pretreated at 573 K for 1 h in an Ar flow at 30 ml $min^{-1}$, then cooled to 373 K and saturated with pure $CO_2$. After that, the sample was purged with Ar for ca. 60 min to remove physically adsorbed $CO_2$ and $CO_2$-TPD was carried out in the range of 323-873 K at a heating rate of 7 K $min^{-1}$. The absorption gas of $NH_3$-TPD measurements was 5% $NH_3$/Ar, other conditions were same as $CO_2$-TPD.

**The constraint index (CI) test**

The constraint index (CI) test was conducted in a fixed-bed micro-reactor (30 cm length, i.d. 4 mm). The typical reactant composition was 50 mol% *n*-hexane and 50 mol% 3-methylpentane. The sample was sieved to collect the 20-40 mesh fractions. Typically, a sample weight of 0.5 g was employed, corresponding to the WHSV of 1.0 $h^{-1}$ and reaction temperature of 603 K in the $N_2$ flow at atmosphere pressure. The products were analyzed using online gas chromatography (HP5890) with a 50 m HP-PLOT/$Al_2O_3$ ‘‘S” capillary column and FID detector. The CI was calculated by the following equation[3] :

$$CI = \frac{\log(1 - X_{n-\text{hexane}})}{\log(1 - X_{3\text{-methylpentane}})}$$

where X denotes the fractional conversion of each species.

**Measurements of catalytic activity**

The prepared catalyst (5.0 g) was sieved to obtain 150-200 $\mu m$ particles and packed into a stainless steel tubular fixed-bed reactor with 1.5 cm inner diameter. Prior to the introduction of reactants, the catalyst was activated in situ in dry $N_2$ flow at 753 K for 2 h and then decreased to the reaction temperature of 698 K. Pre-mixed solution of toluene (T) and methanol (M) with 3 : 1 molar ratio was pumped into the reactor at a weight hourly space velocity (WHSV) of 2.0 $h^{-1}$ with $N_2$ at a flow rate of 20 mL $min^{-1}$. Liquid product was analyzed in a gas chromatograph (Agilent Technologies GC5890) equipped with an INNOWAX capillary column (60 m length, inner diameter 0.25 mm) and a flame ionization detector (FID). Gaseous product was analyzed in another gas chromatograph (GC 5890) equipped with a Carboxen-1000 column and a thermal conductivity detector (TCD).

The conversion of toluene ($C_T$), the selectivity of styrene ($S_{ST}$), and the total selectivity of styrene and ethylbenzene ($S_{ST + EB}$) were estimated by the following equations:

$$C_T\,(\%) = \frac{\text{toluene}_{in} - \text{toluene}_{out}}{\text{toluene}_{in}} \times 100\ \%$$

$$S_{ST}\,(\%) = \frac{\text{styrene}_{out}}{\text{toluene}_{in} - \text{toluene}_{out}} \times 100\ \%$$

$$S_{ST+EB}\,(\%) = \frac{\text{styrene}_{out} + \text{ethylbenzene}_{out}}{\text{toluene}_{in} - \text{toluene}_{out}} \times 100\ \%$$

The normalized reaction rate can be calculated by the following equation:

$$\text{rate}\ (r) = \frac{[\text{toluene}]_{in} x V_{in}}{n_{Cs}}$$

where $[\text{toluene}]_{in}$ is the concentration of toluene in the inlet; *x*, the conversion of toluene within the differential kinetic regime (toluene conversion less than 10%, and not affected by heat or mass transport limitations); $V_{in}$, the total molar flow rate; $n_{Cs}$, the molar quantity of Cs per gram of the catalysts. The apparent activation energy ($E_{app}$) is determined from Arrhenius plots, and tested by tuning the temperature between 663 K and 723 K.

**The transport effect and product inhibition effect**

In order to make sure that the obtained kinetic parameters were not significantly influenced by interphase or intra-particle transfer limitations, the transport effects over Cs-X-FT-15 catalyst were investigated by using Madon-Boudart criterion.[4] Herein, the effect of interphase transport was experimentally evaluated by employing different flow rates of reactants at constant WHSV of 2.0 $h^{-1}$. It was shown in **Figure S10a** that there was no significant change in toluene conversion by varying the flow rate of reactants ( > 10 ml/h). Thus, the interphase diffusion limitation can be

excluded at a feed flow rate of 12 ml/h in this study.

To avoid the internal diffusion, we address the effects of CsOH concentrations (0.3/0.4/0.5/0.6 M) during Cs ion exchange procedures and the resulting changes in Cs loading on toluene reaction rates ( < 15 % toluene conversion). The reaction rates on samples with 23.82, 26.58, 29.67 and 31.44 wt % Cs loading (determined by ICP) showed no significant change (**Figure S10b**). The Cs loading can influence reactivity when diffusional restrictions create intracrystalline gradients of reactants.[5] Consequently, the similar rates normalized per Cs on X-FT-15 sample with 23.82-31.44 wt % Cs loading imply the exclusion of internal diffusion limitation of measured rates in the experimental range.

Ignoring product inhibition when it is in fact present may produce inaccurate kinetic data such as apparent activation energies. Plotting the natural logarithm of toluene conversion versus the natural logarithm of the space time is a simple way to check for product inhibition of styrene in this study. We maintain constant inlet reactant concentrations and vary the space time by changing amount of catalyst (0.5-3 g), while keeping the toluene conversion small. As shown in **Figure S11a**, the slope of the plot is 0.97, which imply that the product inhibition is present but showing small impact in this reaction system.[6, 7] Moreover, the dependence of rate on the concentration of styrene products was investigated (**Figure S11b**). It can be seen that the relatively low concentration of styrene product has little effect on reaction rates.

**Table S1** Texture properties, Si/Al ratio, and CI values of the parent X and $NH_4F$-treated samples

| Samples | $S_{BET}$ [a] ($m^2\ g^{-1}$) | $V_{micro}$ [b] ($cm^3\ g^{-1}$) | $V_{total}$ [c] ($cm^3\ g^{-1}$) | Si/Al [d] | CI Value |
|---|---|---|---|---|---|
| X-P | 702 | 0.29 | 0.34 | 1.3 | 0.5 |
| X-FT-15 | 733 | 0.36 | 0.40 | 1.3 | 1.2 |
| X-FT-30 | 741 | 0.35 | 0.43 | 1.4 | 1.3 |
| X-FT-60 | 714 | 0.23 | 0.39 | 1.7 | 0.6 |

[a] Calculated using BET method.

[b] Calculated using t-plot method.

[c] Calculated at $P/P_0 = 0.99$.

[d] Determined by ICP-AES results.

**Table S2** Comparison of OH groups fractions in supercages and SOD cages via infrared spectra

| Samples | $OH_{SOD}/OH_{SUP}$ |
|---|---|
| X-P | 0.52 |
| X-FT-15 | 0.62 |
| X-FT-30 | 0.54 |
| X-FT-60 | 0.48 |

Calculated by the equation of $OH_{SOD}/OH_{SUP} = (OH_{3550}/\varepsilon_{3550})/(OH_{3640}/\varepsilon_{3640})$. The subtraction IR spectra of dehydrated samples are shown in **Figure 2** and **Figure S5**. Here, the extinction coefficients used for the quantification of OH groups in super cage (3640 $cm^{-1}$) and sodalite cage (3550 $cm^{-1}$) were $\varepsilon(OH)_{3640}$ = 6.76 cm/μmol, and $\varepsilon(OH)_{3550}$ = 5.39 cm/μmol.[8]

**Table S3** Catalytic activities of different Cs-modified catalysts for toluene side-chain alkylation with methanol

| Catalysts | Toluene conversion (%) [a] | Product Selectivity (%) | | | Toluene conversion rates (mmol $_{toluene}$ $mol_{Cs}^{-1}$ $h^{-1}$) | $E_{app}$ (kJ/mol) [c] |
|---|---|---|---|---|---|---|
| | | Styrene | Ethylbenzene | Others [b] | | |
| Cs-X-P | 5.1 | 73.1 | 20.4 | 6.5 | 0.164 | 69.4 ± 1.1 |
| Cs-X-FT-15 | 11.4 | 87.2 | 9.7 | 3.1 | 0.324 | 48.4 ± 1.2 |
| Cs-X-FT-30 | 7.8 | 77.6 | 18.5 | 3.9 | 0.201 | 57.9 ± 0.9 |
| Cs-X-FT-60 | 3.2 | 71.0 | 21.6 | 7.4 | 0.115 | 72.6 ± 3.6 |

Reaction conditions: 698 K, toluene/methanol ratio = 3.0, WHSV = 2.0 $h^{-1}$.

[a] Determined at 1 h time-on-stream.

[b] Other byproducts are mainly xylenes, TMB, and benzene.

[c] The apparent activation energy ($E_{app}$) was tested by tuning the temperature between 663 to 723 K.

**Table S4** Cs content, Cs species states and acid-base properties over different side-chain alkylation catalysts

| Samples | Cs content (wt %) [a] | States of Cs species (%) [b] | | Total Acidity ($\mu$mol $g^{-1}$) [c] | Total Basicity ($\mu$mol $g^{-1}$) [c] |
|---|---|---|---|---|---|
| | | $Cs^+$ | $Cs_2O$ | | |
| Cs-X-P | 23.68 | 78.3 | 21.7 | 80 | 294 |
| Cs-X-FT-15 | 23.82 | 76.8 | 23.2 | 86 | 286 |
| Cs-X-FT-30 | 24.23 | 76.2 | 23.6 | 79 | 290 |

[a] Determined by ICP-AES results.

[b] Determined by XPS results.

[c] Determined by $NH_3$-TPD and $CO_2$-TPD results.

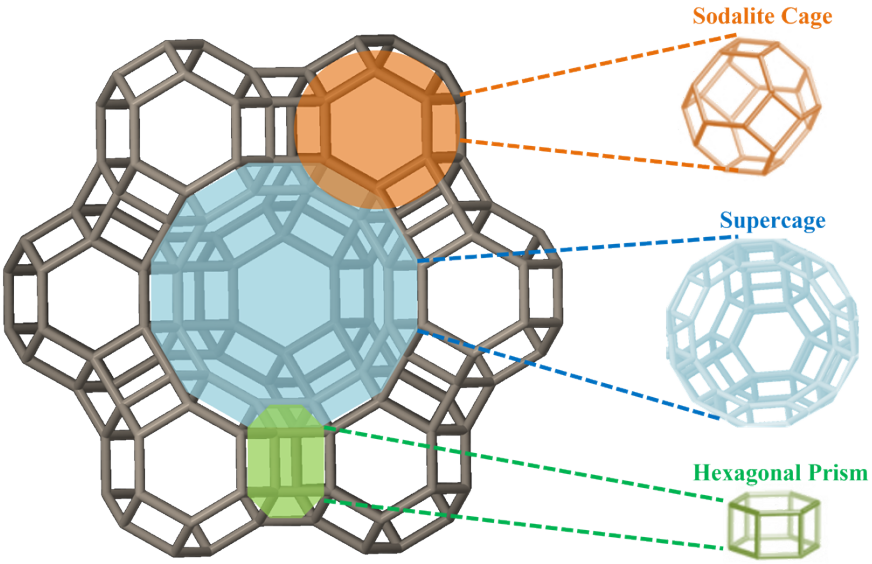


**Scheme S1.** Framework structure of X zeolite (FAU-type). Redrawn based on ref.: *http://www.iza-structure.org/databases*.

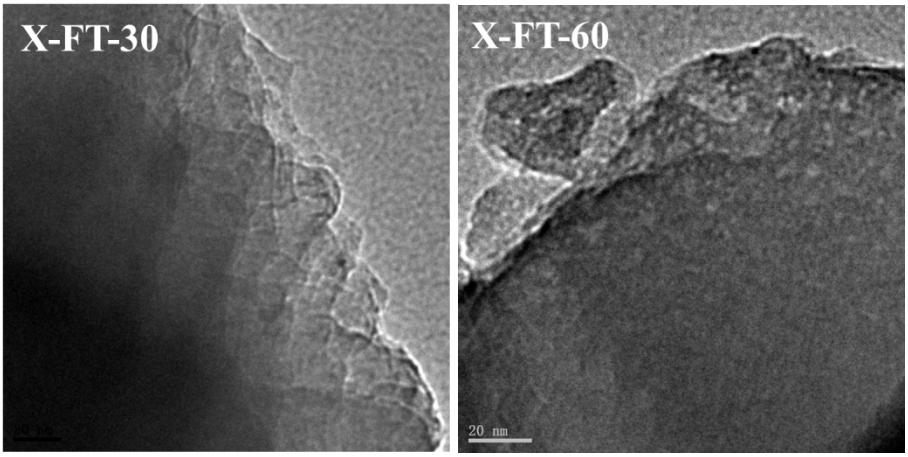


**Figure S1.** TEM images of X-FT-30 and X-FT-60 samples.

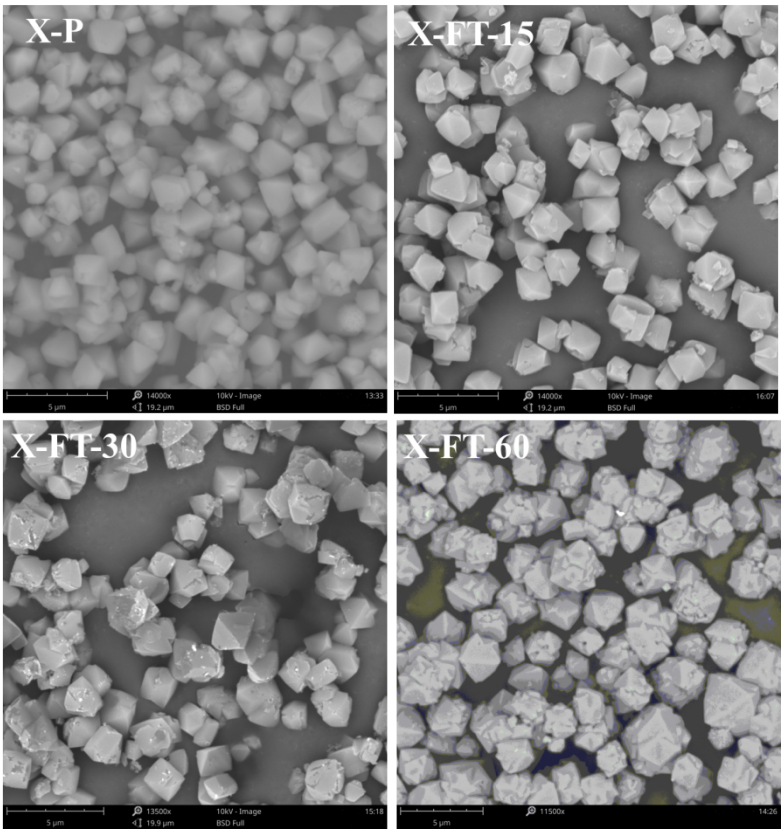


**Figure S2.** SEM images of the parent X and $NH_4F$-treated samples.

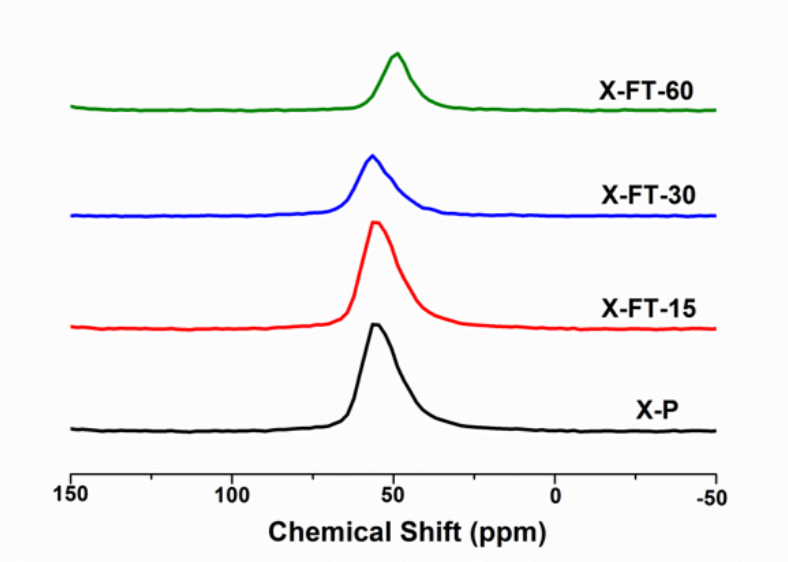


**Figure S3.** $^{27}Al$ MAS NMR spectra of the parent X and $NH_4F$-treated samples.

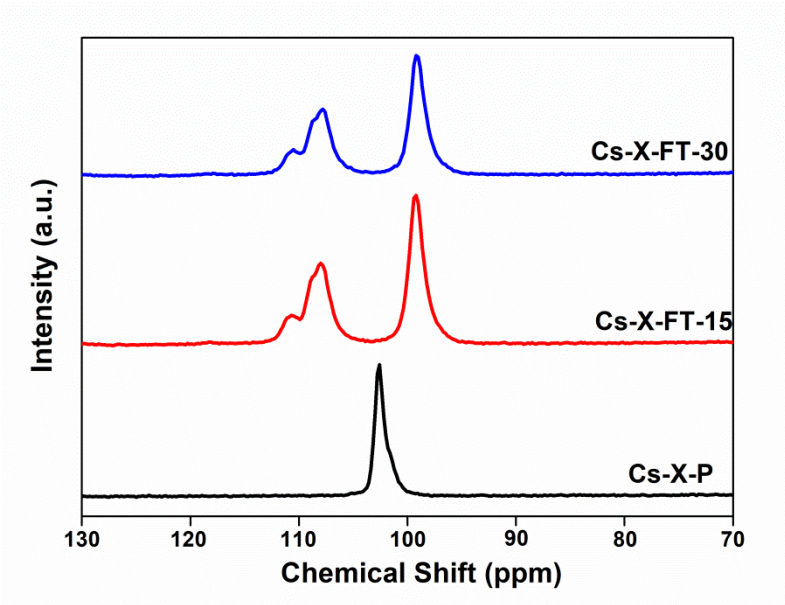


**Figure S4.** $^{129}$Xe MAS NMR spectra of the Cs modified samples recorded at 298 K. Cs-X-FT-15 and Cs-X-FT-30 present two peaks corresponding to SOD cages (high chemical shift) and supercages (low chemical shift) while Cs-X-P show only one peak corresponding to supercages.

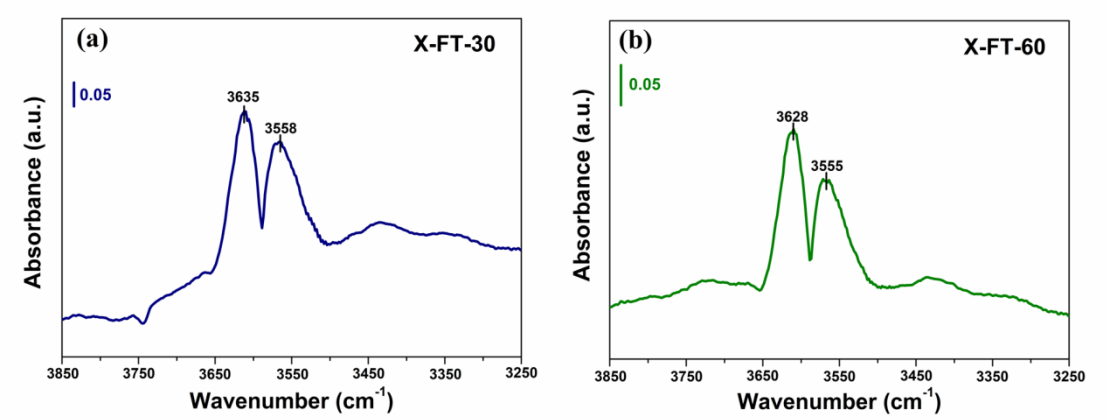


**Figure S5.** The IR spectra of dehydrated (a) X-FT-30 and (b) X-FT-60 samples

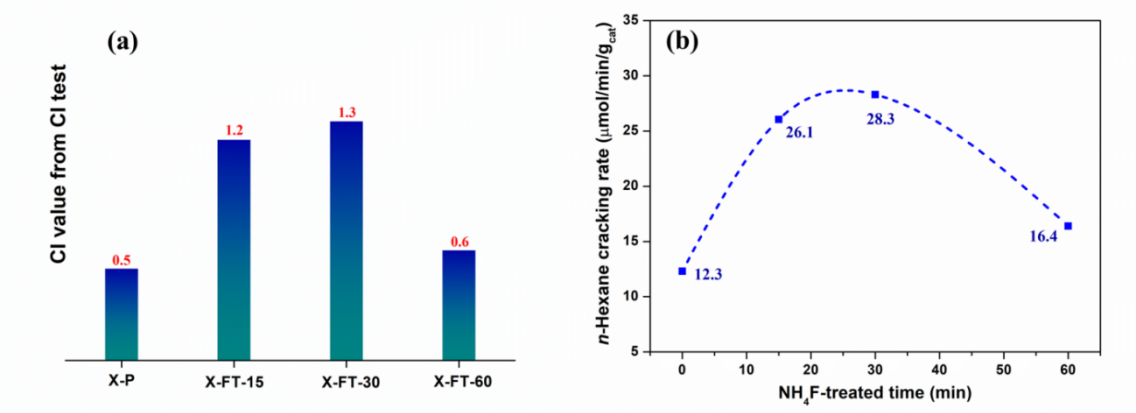


**Figure S6.** (a) CI values and (b) *n*-hexane cracking rates on X-P and derivatives $NH_4F$ treated for 15, 30, and 60 min.

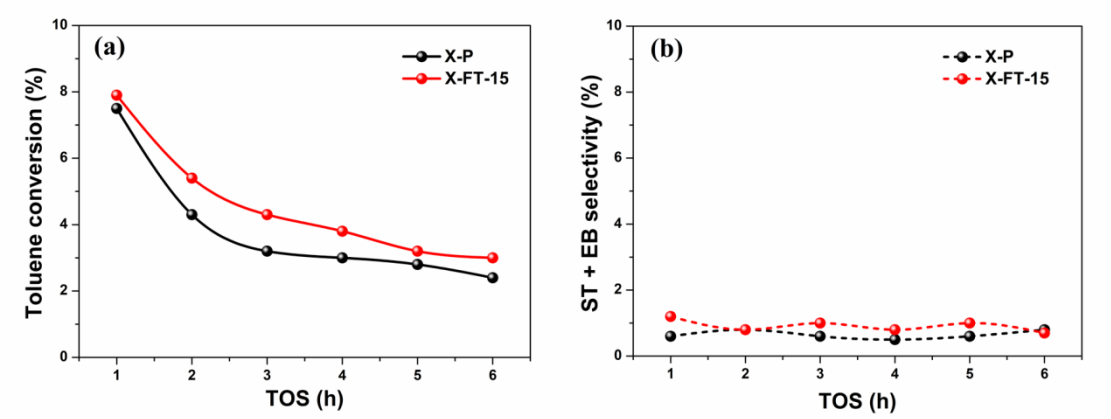


**Figure S7.** Conversion of toluene and total selectivity of styrene and ethylbenzene for side-chain alkylation reaction over X-P and X-FT-15 samples. Reaction conditions: 698 K, toluene/methanol ratio = 3.0, WHSV = 2.0 $h^{-1}$.

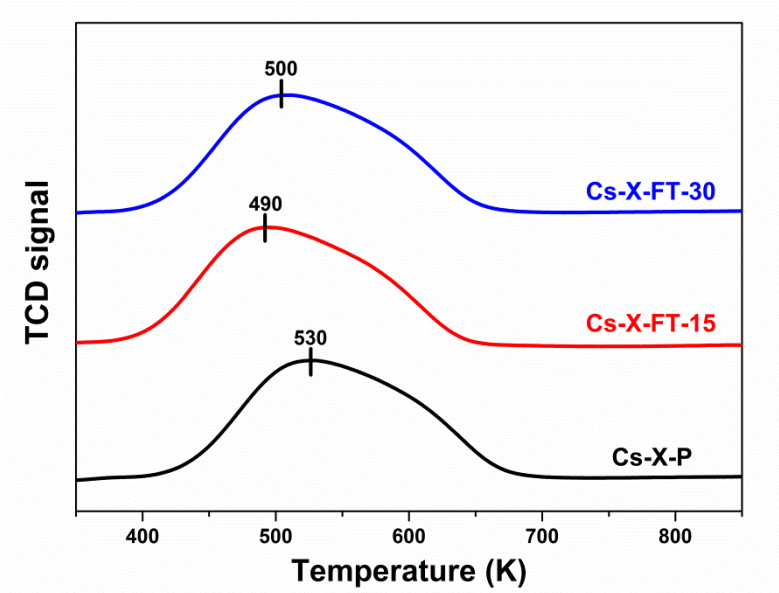


**Figure S8.** $CO_2$-TPD profiles of the Cs-X-P, Cs-X-FT-15 and Cs-X-FT-30 catalysts

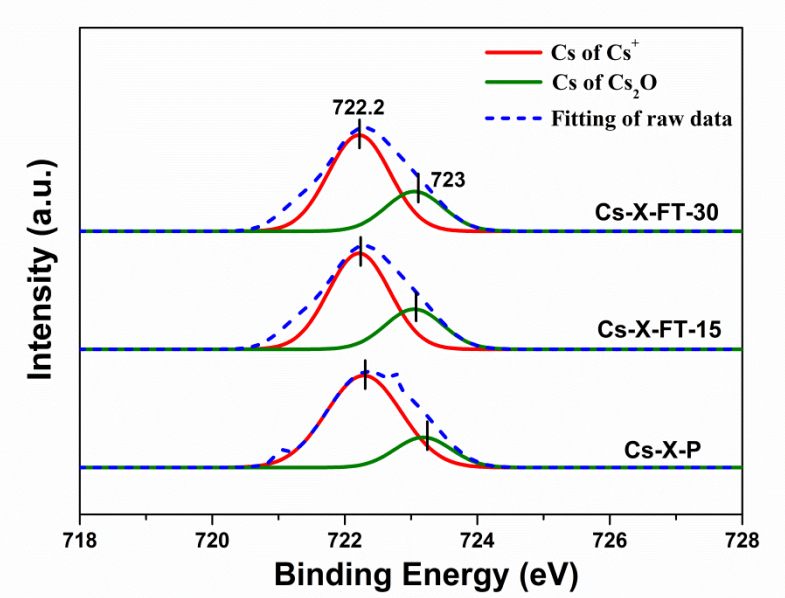


**Figure S9.** Cs $3d_{5/2}$ XPS signals of Cs-X-P, Cs-X-FT-15 and Cs-X-FT-30 catalysts. Each catalyst shows two Cs $3d_{5/2}$ peaks, indicating the existence of two kinds of Cs species: the peak centred at around 722.2 eV was attributed to $Cs^+$, while the other signal ranged from 723.0 to 723.2 eV was assigned to $Cs_2O$ species.[9, 10]

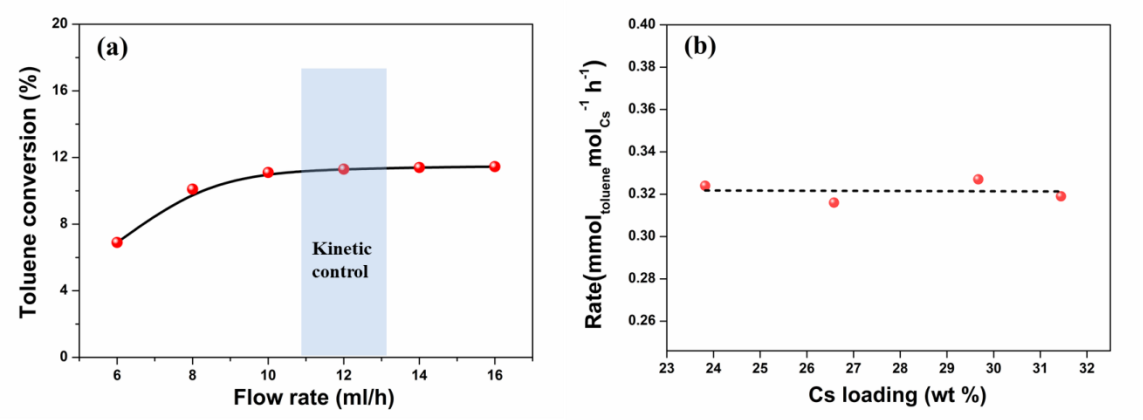


**Figure S10.** (a) variation of toluene conversion with the flow rate of reactants on Cs-X-FT-15 catalyst (tuning the catalyst mass from 2.5 g to 6.25 g to achieve different reactants flow rates at constant WHSV of 2.0 $h^{-1}$) and (b) variation of toluene reaction rates with the Cs loading on Cs-X-FT-15 catalyst (tuning CsOH concentrations from 0.3M to 0.6 M during Cs ion exchange procedures).

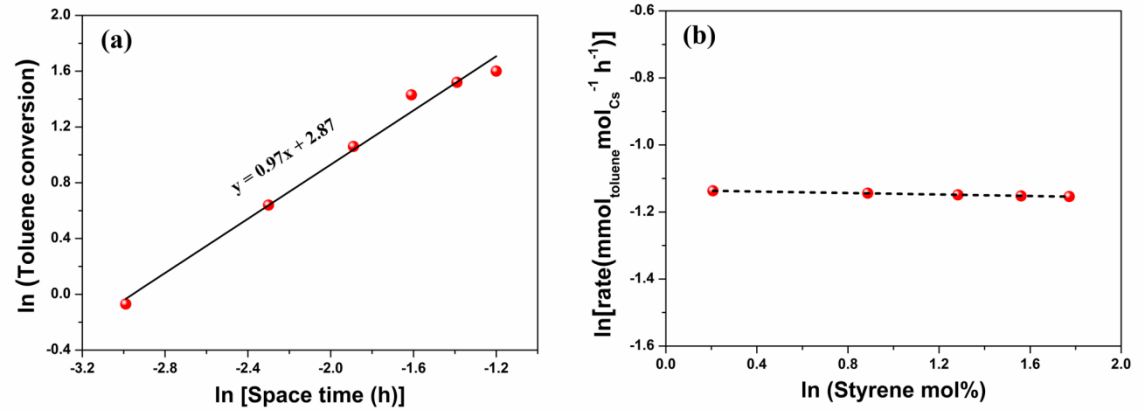


**Figure S11.** (a) natural log of toluene conversion as a function of the natural log of space time and (b) the dependence of toluene conversion rate on the concentration of styrene products (1.23-5.88 mol%).

## References:

(1) Thibault-Starzyk, F.; Gil, B.; Aiello, S.; Chevreau, T.; Gilson, J. P.; In situ thermogravimetry in an infrared spectrometer: an answer to quantitative spectroscopy of adsorbed species on heterogeneous catalysts. *Micropor. Mesopor. Mater.* 2004, *67*, 107-112.

(2) Tomar, D.; Kaur, H.; Rana, B.; Talegaonkar, K.; Maharana, V.; Jena, K. C. In Advances in Spectroscopy: Molecules to Materials (*Eds.: D. K. Singh, S. Das, A. Matern*y), Springer Singapore, Singapore, 2019, pp. 3-21.

(3) Carpenter, J. R.; Yeh, S.; Zones, S. I.; Davis, M. E. Further investigations on Constraint Index testing of zeolites that contain cages. *J. Catal.* 2010, *269*, 64-70.

(4) Madon, R. J.; Boudart, M. Experimental criterion for the absence of artifacts in the measurement of rates of heterogeneous catalytic reactions. *Ind. Eng. Chem. Fundament.* 1982, *21*, 438-447.

(5) Sarazen, M. L. Doskocil, E.; Iglesia, E. Catalysis on solid acids: Mechanism and catalyst descriptors in oligomerization reactions of light alkenes, *J. Catal.* 2016, *344*, 553-569.

(6) Harris, J. W.; Bhan, A.; Moderation of chlorine coverage and ethylene epoxidation kinetics via ethane oxychlorination over promoted Ag/alpha-$Al_2O_3$. *J. Catal.* 2018, *367*, 62-71.

(7) Harris, J. W.; Arvay, J.; Mitchell, G.; Delgass, W. N.; Ribeiro, F. H. Propylene oxide inhibits propylene epoxidation over Au/TS-1, J. Catal. 2018, *365*, 105-114.

(8) Qin, Z. X.; Cychosz, K. A.; Melinte, G.; El Siblani, H.; Gilson, J. P.; Thornmes, M.; Fernandez, C.; Mintova, S.; Ersen, O.; Valtchev, V. Opening the Cages of Faujasite-Type Zeolite. *J. Am. Chem. Soc*. 2017, *139*, 17273-17276.

(9) Podgornov, E. A.; Prosvirin, I. P.; Bukhtiyarov, V. I. XPS, TPD and TPR studies

of Cs-O complexes on silver: their role in ethylene epoxidation, *J. Mol. Catal. A: Chem.* 2000, *158*, 337-343.

(10) Larichev, Y. V.; Moroz, B. L.; Zaikovskii, V. I.; Yunusov, S. M.; Kalyuzhnaya, E. S.; Shur, V. B.; Bukhtiyarov, V. I. XPS and TEM studies on the role of the support and alkali promoter in Ru/MgO and Ru-$Cs^{+}$/MgO catalysts for ammonia synthesis. *J. Phys. Chem. C* 2007, *111*, 9427-9436.